

## Metal Complexation with Langmuir Monolayers of Histidyl Peptide Lipids

Qun Huo,<sup>[a]</sup> Guodong Sui,<sup>[a]</sup> Yujun Zheng,<sup>[a]</sup> Peter Kele,<sup>[a]</sup> Roger M. Leblanc,<sup>\*,[a]</sup> Takeshi Hasegawa,<sup>[b]</sup> Jujiro Nishijo,<sup>[b]</sup> and Junzo Umemura<sup>[c]</sup>

**Abstract:** Langmuir monolayers made from peptide-lipid molecules represent a novel direction in the research areas of biomimetic interfaces and two-dimensional supramolecular chemistry. Peptide structures and molecular recognition activities toward other guest molecules have been the focus of previous study. This study reports the investigation of metal complexation to histidine-containing peptide lipids in the organized Langmuir, Langmuir–Schaefer, or Langmuir–Blodgett films. Three peptide lipids **PEP1**–**PEP3**, with a histidine amino acid incorporated in the middle of the peptide, were designed and synthesized. The monolayer structures and

metal-binding activities of each peptide lipid and their 1:1:1 molar ratio mixture were studied by thermodynamic and spectroscopic techniques. It was found that hard Lewis acid type metal cations such as  $K^+$  and  $Mg^{2+}$ , and borderline or soft metal cations such as  $Zn^{2+}$ ,  $Cu^{2+}$ , and  $Cd^{2+}$  exhibit clearly different binding activity toward peptide-lipid monolayers. The conformational changes of peptides upon binding with  $Cu^{2+}$  and  $Zn^{2+}$  were partially revealed by FT-IR

spectroscopic studies. Furthermore, by adding a fluorescent-probe lipid to the peptide monolayer, dramatic fluorescence change was observed when  $Cu^{2+}$  or  $Zn^{2+}$  bound to the Langmuir and Langmuir–Schaefer films of peptide-lipid monolayers. Metal–protein complexation plays a crucial role in the function and activity of proteins and enzymes. Investigation of metal complexation to organized peptide Langmuir monolayers may provide an alternative approach for the development of artificial metalloproteins and novel supramolecular systems or materials.

**Keywords:** air–water interface • metal complexation • monolayers • peptides • surface chemistry

## Introduction

Like the study of proteins and protein-lipid interactions at the air–water interface,<sup>[1,2]</sup> peptide structures and peptide-lipid interactions at the air–water interface have also been of great interest to chemists in the past.<sup>[3–7]</sup> However, it is only recently that Langmuir and Langmuir–Blodgett films of synthetic peptides with hydrophobic alkyl tails have arisen as a novel direction for research, particularly in the areas of biomimetic interfaces and two-dimensional supramolecular chemistry. Different from previous research, this new direction focuses on the assembling process of single, synthetic peptide lipids into supramolecular species with designed structures and

functions. A few representative works are worthy of particular mention here. Kunitake's group started the investigation of molecular recognition at the air–water interface between functional Langmuir monolayers and their guest molecules, which included peptide-lipid monolayers with small peptide guest molecules.<sup>[8–11]</sup> Fields et al. were more interested in the collagen-like triple-helix structures of peptide-lipid amphiphiles assembled in Langmuir and Langmuir–Blodgett films, and their applications as artificial biointerfaces.<sup>[12,13]</sup> On the other hand, Leblanc's group focused on the surface-chemistry technique itself, and recently reported, for the first time, the application of combinatorial library techniques to Langmuir monolayer studies.<sup>[14]</sup> Instead of using one or a few limited lipid molecules, as in the traditional approach, a peptide-lipid library was used for monolayer formation. Due to the increase in molecular diversity in a monolayer, the probability of finding a matching molecular recognition system for the guest molecules in which you are interested is greatly increased.

The aforementioned previous work, as well as many other studies on peptide monolayers and peptide-lipid interactions, has been mainly focused on the molecular structures and interactions between peptide-lipid monolayers and guest molecules. In contrast, reports of metal complexation with peptide lipids in the mobile Langmuir monolayer is very rare.

[a] Prof. R. M. Leblanc, Dr. Q. Huo, G. Sui, Y. Zheng, P. Kele  
Center for Supramolecular Science, Department of Chemistry  
University of Miami, 1301 Memorial Drive Cox 315  
Coral Gables, FL 33124 (USA)  
Fax: (+1) 305-284-1880  
E-mail: rml@umiami.ir.miami.edu

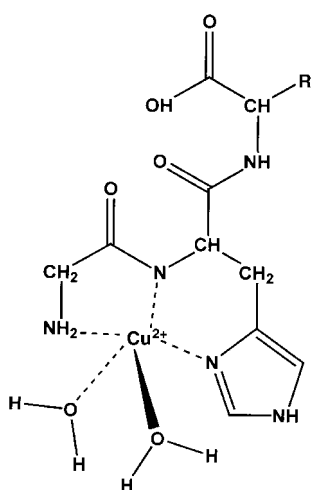
[b] Prof. Dr. T. Hasegawa, Prof. Dr. J. Nishijo  
Kobe Pharmaceutical University, Motoyama-kita  
Higashinada-ku, Kobe, 658-8558 (Japan)

[c] Prof. Dr. J. Umemura  
Institute for Chemical Research, Kyoto University  
Uji, 611-0011 (Japan)

Ringsdorf et al. studied metal complexation with a chiral imidazole amphiphile in Langmuir monolayers.<sup>[15]</sup> However, since the polar group only contains an imidazole group and lacks peptide bonds, this imidazole lipid does not represent the typical features of peptide lipids at the air–water interface. In the middle 1990s, Tampé et al. synthesized a class of chelator lipids bearing a nitrilotriacetic acid head group connected to a hydrocarbon chain through the amino acid lysine.<sup>[16]</sup> Thin films of these lipids were found to be highly sensitive toward nickel ions; they form complexes and thereby generate binding sites for histidine-tagged fusion proteins. The nickel ions were known to complex with the three carboxylic groups from the lipids and the imidazole group from the histidine amino acid. This type of lipid is essentially a small organic ligand to nickel ions, not a typical peptide.

A main goal of this study is to investigate metal complexation with small peptide lipids at the air–water interface. Moreover, the study of peptide–metal complexation also has general significance for the development of chemical- and biosensors for the detection of metal cations. Despite the fact that many chemical or peptide–metal complexes have been discovered that can be used for chemical sensors, research in this field remain active due to the need for more sensitive and specific molecules and materials for biologically important metal cations.<sup>[17–21]</sup> As an ideal immobilization technique, Langmuir–Blodgett film-based peptide–metal complex systems may be used directly for chemo- and biosensor fabrication.

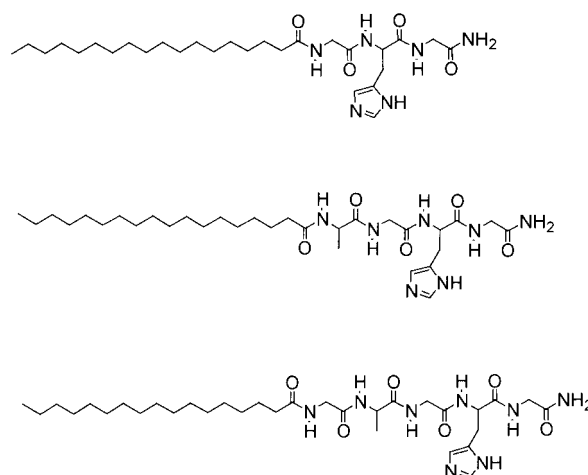
Histidine is one of the most common amino acid ligands for the metal cations  $\text{Cu}^{2+}$  and  $\text{Zn}^{2+}$  through its imidazole nitrogen atom. A few histidine-containing small peptides such as GlyHisGly or GlyGlyHis<sup>[22–24]</sup> and GlyHisLys<sup>[25–28]</sup> are known to form complexes with  $\text{Cu}^{2+}$  with high binding constants through a similar binding motif to that illustrated in Scheme 1. In this binding motif, the amino group from the N-terminal glycine is known to be necessary for metal complexation. We previously noticed that if this amino group is derived with a certain functional group such as nitro-cinnamic acid, the molecule loses its copper-binding activity in



Scheme 1. A common binding motif between a few small tripeptides and  $\text{Cu}^{2+}$ . The shaded N-terminal amino group from glycine is an essential element for the coordination with  $\text{Cu}^{2+}$  in solution.

aqueous solution. However, no study has been done to test the metal-binding activity of these tripeptides at the air–water interface, when the N-terminal is linked with a hydrophobic alkyl chain. Conformational changes in proteins upon adsorption to interfaces is a well-known phenomenon observed by surface chemists.<sup>[1, 2, 29]</sup> There are enough reasons for speculating that hydrocarbon-derived peptide lipids may exhibit different behavior toward metal complexation at the air–water interface than in aqueous solution.

In this study, we chose GlyHisGly as the metal-binding moiety and stearic acid as the hydrophobic long-tail moiety. It has to be mentioned that we designed and synthesized three peptide lipids **PEP1** to **PEP3** each containing a GlyHisGly moiety, the second one with an extra alanine, and the third one with two extra amino acids: glycine and alanine (Scheme 2). The purpose was to extend the length of the



Scheme 2. Structures of histidine-containing peptide lipids used in the present monolayer study. From top to bottom: **PEP1** C18-GlyHisGly- $\text{NH}_2$ , **PEP2** C18-AlaGlyHisGly- $\text{NH}_2$ , **PEP3** C18-GlyAlaGlyHisGly- $\text{NH}_2$ .

peptides and to see the difference between their monolayer and metal-binding properties. Originally, a second purpose behind this design was to see, in case a single peptide lipid could not form the desired structure for metal complexation, whether the mixture of these three peptide lipids could accomplish the same goal through the combination of amino acid ligand histidines from different peptides; an idea based on the combinatorial surface-chemistry concept proposed earlier.<sup>[14]</sup> During the study, we found that the mixed-peptide-lipid monolayer exhibits almost the same properties and metal binding activities as each single peptide lipid. The long-term goal of this research is to investigate the molecular recognition and metal-complexation activity of mixed-peptide lipids, even peptide-lipid libraries, in Langmuir monolayers. Therefore, most of the experimental results presented and discussed here are the results of the 1:1:1 molar ratio mixed-peptide-lipid monolayer of **PEP1** to **PEP3**.

## Results and Discussion

The peptide lipids were synthesized according to standard solid-phase peptide synthesis by using Fmoc chemistry.<sup>[30]</sup>

Rink resin was used for the peptide synthesis so that we could obtain peptides with carboxamide end groups. Originally, Wang resin has been used for peptide synthesis and the peptides thus obtained have a free carboxylic acid end group. This carboxylic acid end group (pK<sub>a</sub> around 3.0) is negatively charged in pure water with a pH near neutral, and we were concerned that metal cations would exhibit electrostatic interactions with the peptide lipids instead of metal–ligand complexation. Therefore, Rink resin was used to avoid this problem. The carboxamide group remains uncharged under the experimental conditions used in this study.

**Surface pressure–area isotherms:** The surface pressure–area isotherms of each peptide and of the 1:1:1 mixture of the three peptides were measured in a pure water subphase. In general, it was observed that all three lipids and their mixture form stable monolayers at the air–water interface in this subphase (Figure 1). The limiting molecular areas obtained for three

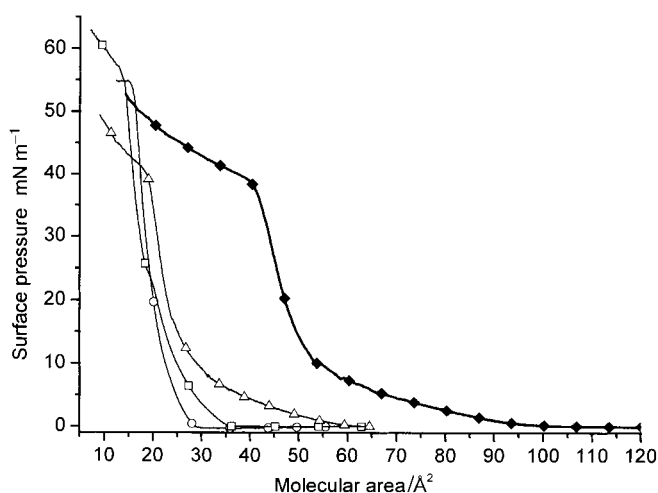


Figure 1. The surface pressure–area isotherms of peptide lipids **PEP1** to **PEP3** and their 1:1:1 molar ratio mixture in a pure water subphase (pH 5.8,  $20 \pm 1^\circ\text{C}$ );  $\circ$  **PEP1**,  $\square$  **PEP2**,  $\triangle$  **PEP3**,  $\blacklozenge$  mixture.

peptides are close to each other at around  $25 \text{ \AA}^2$  per molecule; this is approximately equivalent to the cross-section of one alkyl chain. However, the shape of each isotherm varies slightly from one to the other. The surface pressure starts to lift with larger molecular area, compare the **PEP3** with the **PEP2** and the **PEP2** with the **PEP1** monolayer. While **PEP1** exhibits a clear solid condensed phase, a kink point was found for the **PEP2** and **PEP3** monolayers at around  $22 \text{ \AA}^2$  per molecule; this indicates the collapse of the monolayers at this stage. These differences should be due to the lengths of the peptides on the lipids. For the mixture sample, the monolayer changes from a liquid expanded phase within a large molecular area range to a liquid condensed phase until it collapses at a relatively low surface pressure relative to the single peptide-lipid monolayer. The limiting molecular area of the mixed monolayer is approximately the sum of three peptide-lipid monolayers.

To examine the binding behavior of peptide-lipid monolayers with metal cations, we chose three types of metals to study: hard Lewis acids such as  $\text{K}^+$ ,  $\text{Mg}^{2+}$ , soft Lewis acids

such as  $\text{Cd}^{2+}$ , and borderline Lewis acids including  $\text{Cu}^{2+}$  and  $\text{Zn}^{2+}$ . According to hard Lewis acid–hard base and soft Lewis acid–soft base rules,  $\text{Cu}^{2+}$  and  $\text{Zn}^{2+}$  should exhibit the highest degree of complexation with the peptide-lipid monolayer, since the imidazole nitrogen on histidine is a borderline base.<sup>[31]</sup>

Subphases containing different concentrations of metal salts were prepared and adjusted to approximately pH 6.0 before monolayer formation. The surface pressure–area isotherms of each peptide lipid and the 1:1:1 molar ratio mixture monolayer in these subphases were measured. Since each single peptide lipid and the mixture all exhibit very similar isotherm changes in different subphases, only the results of the mixed-peptide-lipid monolayer are shown here (Figure 2). From surface pressure–area isotherm measurements, one can see that in subphases with hard Lewis acid type cations such as  $\text{K}^+$  and  $\text{Mg}^{2+}$ , the molecular areas of the monolayer exhibit no or a very slight increase compared with

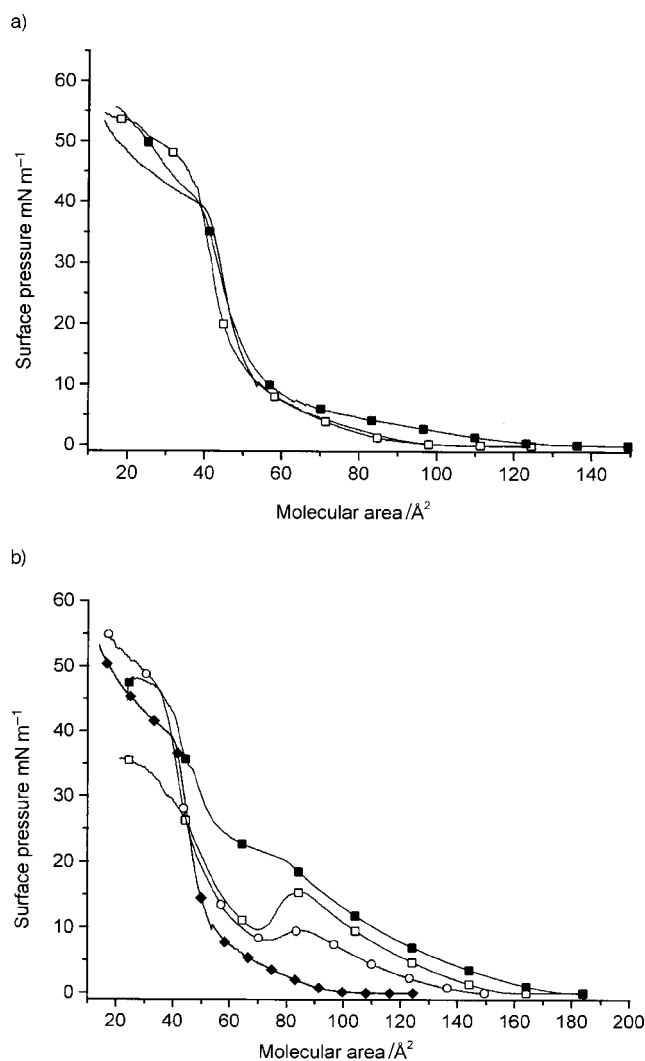


Figure 2. The surface pressure–area isotherms of 1:1:1 molar ratio mixed-peptide-lipid monolayers in subphases with the presence of different metal cations. All the subphases containing metal cations were adjusted to  $\approx \text{pH } 6.0$  prior to measurement. a) Hard Lewis acid type cations:  $\blacklozenge$  water,  $\square$   $\text{KCl } 10 \text{ mM}$ ,  $\blacksquare$   $\text{MgCl}_2 \text{ } 10 \text{ mM}$ . b) Borderline (soft) Lewis acid type cations:  $\blacklozenge$  water,  $\square$   $\text{ZnCl}_2 \text{ } 1 \text{ mM}$ ,  $\blacksquare$   $\text{CuCl}_2 \text{ } 1 \text{ mM}$ ,  $\circ$   $\text{CdCl}_2 \text{ } 10 \text{ mM}$ .

the pure water subphase (Figure 2a). In contrast, in subphases with borderline (hard-soft) metal cations such as  $\text{Cu}^{2+}$  and  $\text{Zn}^{2+}$ , the area per molecule of the monolayer significantly increased compared with the pure water subphase (Figure 2b). The maximum molecular area expansion reaches as high as  $80 \text{ \AA}^2$  per molecule at the surface pressure lifting point in the subphase with  $\text{Cu}^{2+}$  compared with the pure water subphase, even at a  $\text{Cu}^{2+}$  concentration of  $1 \text{ mM}$ . Furthermore, it was found that with soft metal cations such as  $\text{Cd}^{2+}$  present in the subphase, the molecular area is also significantly expanded; although with less expansion than that found for  $\text{Zn}^{2+}$  and  $\text{Cu}^{2+}$  subphases. At the same concentration,  $\text{Cu}^{2+}$  causes greater expansion than  $\text{Zn}^{2+}$  ( $1 \text{ mM}$ ), and  $\text{Zn}^{2+}$  causes greater expansion than  $\text{Cd}^{2+}$  ( $10 \text{ mM}$ ). The molecular area expansion follows the order  $\text{Cu}^{2+} > \text{Zn}^{2+} > \text{Cd}^{2+} \gg \text{K}^+$  and  $\text{Mg}^{2+}$ . According to the hard–soft acid–base matching rule, the sequence for different metal cations to form complexes with the imidazole group from histidine is expected to be  $\text{Cu}^{2+}$ ,  $\text{Zn}^{2+} > \text{Cd}^{2+} \gg \text{K}^+$  and  $\text{Mg}^{2+}$ .<sup>[31]</sup> The binding activity of the peptide monolayer toward different metal cations observed from isotherm measurements matches very well with the hard and soft acid–base rule. From this experimental result, we may suggest that it is very likely that the monolayer uses the imidazole groups or the amide nitrogens from peptides to coordinate with their matching metal cations.

**FT-IR spectroscopic study of metal complexation within Langmuir–Blodgett films:** The interaction between  $\text{Cu}^{2+}$  and  $\text{Zn}^{2+}$  cations and the mixed-peptide monolayer was further characterized by FT-IR spectroscopy. FT-IR spectra of one-layer Langmuir–Blodgett films of mixed-peptide monolayers deposited on a gold-evaporated glass slide from pure water,  $\text{ZnCl}_2$  ( $10^{-5} \text{ M}$ ) and  $\text{CuCl}_2$  ( $10^{-5} \text{ M}$ ) subphases at different surface pressures were recorded (Figure 3a to c). Of particular interest for the analysis of the secondary structure of peptides and proteins are, inter alia, the amide I band at  $1600$ – $1750 \text{ cm}^{-1}$ , amide II band around  $1500$ – $1600 \text{ cm}^{-1}$ , and amide III band around  $1200$ – $1350 \text{ cm}^{-1}$ ; these can all be found in the spectra of the peptide monolayer in three subphases. Analysis of the peptide structures of Langmuir and Langmuir–Blodgett (LB) films by using FT-IR spectroscopy remains challenging due to complications from the techniques used to measure spectra at the air–water interface or LB films compared with the work done in free solution. All three amide bands, plus the amide A band, can be used to assign peptide secondary structures, as reported.<sup>[5, 6]</sup> However, from our study, we particularly found that structural analysis through comparison of amide I and amide III can bring a much clearer assignment.<sup>[32a]</sup> The results are discussed below.

In the peptide monolayer from the pure water subphase, the amide I band changes its position from  $1689$  to  $1691 \text{ cm}^{-1}$  when the surface pressure is increased from  $7$  to  $25 \text{ mN m}^{-1}$  (Figure 3a), which is not significant. The amide I band around  $1690 \text{ cm}^{-1}$  is an indication of antiparallel pleated-sheet structure.<sup>[32a]</sup> Therefore, from this band, it may be suggested that peptides adopt an antiparallel  $\beta$ -sheet structure in the monolayer. This conclusion was further supported by the appearance of an amide III vibration band at  $1240 \text{ cm}^{-1}$ , which is a typical amide III band for  $\beta$ -sheets.<sup>[32a,b]</sup> A smaller band

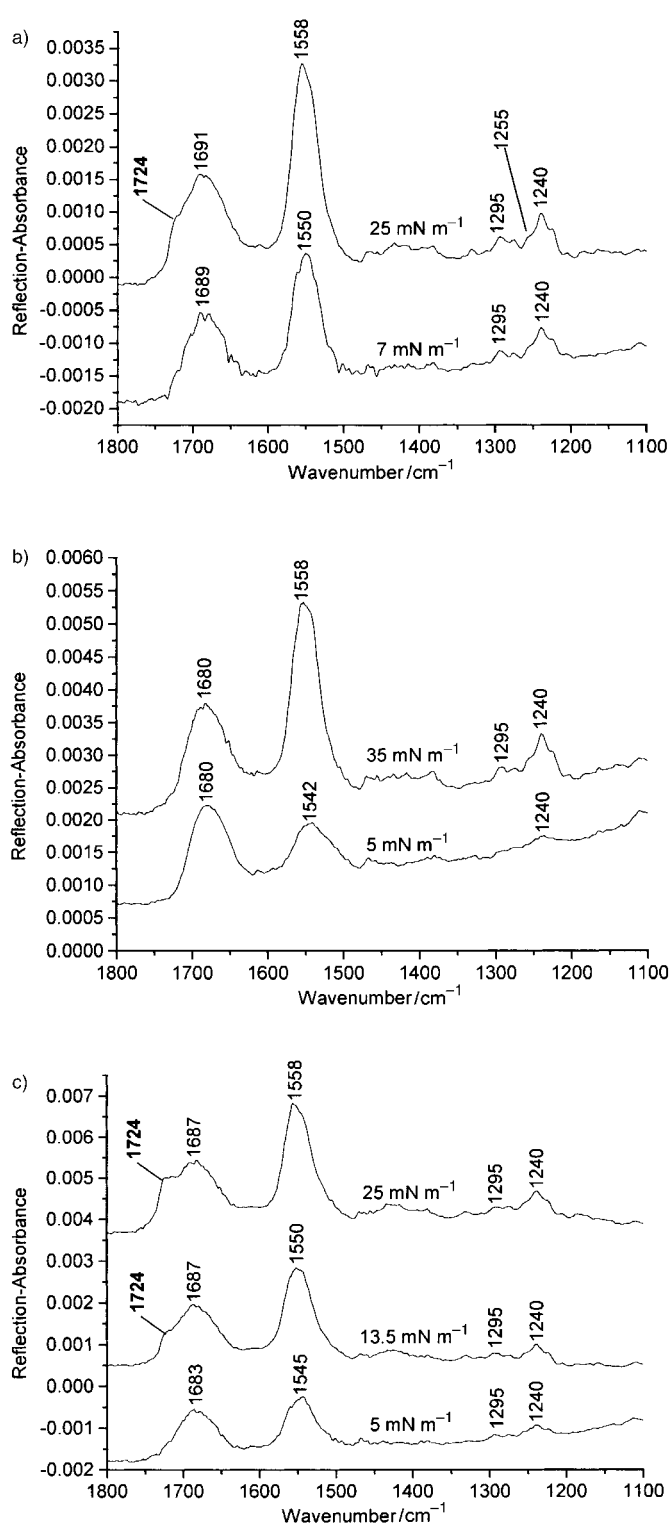


Figure 3. FT-IR spectra of one-layer Langmuir–Blodgett films of mixed-peptide-lipid monolayers deposited from different subphases at different surface pressures: a) pure water, b)  $\text{Cu}^{2+}$  ( $10^{-5} \text{ M}$ ), c)  $\text{Zn}^{2+}$  ( $10^{-5} \text{ M}$ ).

around  $1295 \text{ cm}^{-1}$  suggests that unordered structure also exists in the peptide monolayer. A very small band at  $1255 \text{ cm}^{-1}$  supports the coexistence of  $\beta$ -sheet and unordered structures. In contrast to what happens in free solution, short peptide lipids tend to form  $\beta$ -sheet-like structures at the air–water interface. This phenomenon was also noticed by

Kunitake's group during the study of dipeptide-lipid monolayers.<sup>[10, 11]</sup>

Another interesting point in the IR spectra of peptide monolayers from the pure water subphase is the appearance of a new band at  $1724\text{ cm}^{-1}$  at a high surface pressure. It is generally recognized that the amide I band derived from proteins appears at wavenumbers lower than  $1700\text{ cm}^{-1}$  due to the extensive hydrogen bonding between amide and water molecules. Theoretical calculation gives the non-hydrogen-bonded amide I vibration band at approximately  $1720\text{ cm}^{-1}$ .<sup>[32c]</sup> For the peptide monolayer studied here, it is possible that, at low surface pressure, the peptide moieties including all C=O groups are embedded in the water phase. Hydrogen bonding is present between C=O groups and water molecules; this leads to the observed vibration band at the relatively low wavenumber of  $1690\text{ cm}^{-1}$ . With increased surface pressure, part of the peptide moieties may be pushed to the air, that is, some C=O groups may leave the water phase and become oriented toward air. If this occurs, the C=O groups are no longer hydrogen bonded with water molecules; this leads to the observed vibration band at the much higher wavenumber of  $1724\text{ cm}^{-1}$ .

When  $\text{Cu}^{2+}$  cations bind to the monolayer, a structural change in the peptides compared with the LB film from the pure water subphase can be clearly seen from its IR spectra (Figure 3b). At the low surface pressure of  $5\text{ mNm}^{-1}$ , the amide I band appears at  $1680\text{ cm}^{-1}$ , approximately  $10\text{ cm}^{-1}$  lower than that found in the pure water subphase. It is known that the antiparallel  $\beta$ -sheet structures of proteins give vibration bands at higher wavenumbers around  $1690\text{ cm}^{-1}$ , while turn structures give vibration bands at slightly lower wavenumbers around  $1680\text{ cm}^{-1}$ , and  $\alpha$ -helices normally lead to vibration bands at around  $1640\text{ cm}^{-1}$ .<sup>[32a,b]</sup> Although overlapping can be often found in the vibration bands of  $\beta$ -sheet and turn structures, as far as the IR spectra of the peptide monolayer in the pure water subphase is concerned, it is more reasonable to assign this band at  $1680\text{ cm}^{-1}$  to the turn structure of peptides in the monolayer. Checking more closely, the amide III vibration region, the band at  $1240\text{ cm}^{-1}$  corresponding to  $\beta$ -sheet structures, is almost negligible until a high surface pressure of  $35\text{ mNm}^{-1}$  is reached; this suggests the disappearance of  $\beta$ -sheets in the monolayer upon binding with  $\text{Cu}^{2+}$ . Similar to that found on the LB film of peptide monolayers from the pure water subphase, unordered structure may also exist in this peptide/ $\text{Cu}^{2+}$  monolayer, since a small band at around  $1295\text{ cm}^{-1}$  can be identified.

Of more interest is that the band at  $1724\text{ cm}^{-1}$  observed for the pure water subphase at high surface pressure never appears in the spectra of peptide/ $\text{Cu}^{2+}$  monolayer. This dramatic difference may be attributed to the conformational change in peptides in the monolayer upon binding with  $\text{Cu}^{2+}$ . Complexation between the  $\text{Cu}^{2+}$  and peptide moieties leads to disruption of the  $\beta$ -sheets and the formation of turn structures, or even unordered structures. This turn or unordered structure possibly maximizes the hydrogen bonding between peptides and water molecules, so as to keep the peptide moieties inside water phase without being pushed into the air phase even at high surface pressure. From the character-

ization of LB films, the structural difference between the  $\text{Cu}^{2+}$ -bound and unbound peptide-lipid monolayers at the air–water interface may be expressed with a model as shown in Figure 4.

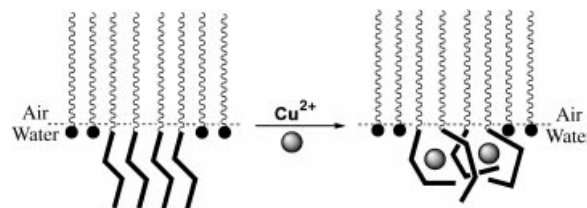


Figure 4. A model to illustrate the structural change of the mixed-peptide-lipid monolayer upon binding with  $\text{Cu}^{2+}$  cations at the air–water interface.

On the other hand, when  $\text{Zn}^{2+}$  is present in the subphase at the low concentration of  $10^{-5}\text{ M}$ , the IR spectra of the mixed-peptide-lipid monolayers exhibit only some slight differences from those of the pure water subphase (Figure 3c). Tracing the amide I band, it was found that at low surface pressure this band appears at  $1683\text{ cm}^{-1}$ , slightly lower than that found for the pure water subphase. The amide III bands corresponding to unordered and  $\beta$ -sheet structures appear at  $1295$  and  $1240\text{ cm}^{-1}$ , respectively. Then at higher surface pressure, from  $13.5\text{ mNm}^{-1}$ , a new band also appears at higher wavenumber around  $1724\text{ cm}^{-1}$ . This means that, with the presence of  $\text{Zn}^{2+}$  in the subphase at a concentration of  $10^{-5}\text{ M}$ , the binding of  $\text{Zn}^{2+}$  to the monolayer is not strong enough to hold the peptide in water subphase at high surface pressure. It seems that the binding of  $\text{Zn}^{2+}$  to the peptide monolayer at low concentration does not alter the secondary structure of the peptide significantly. The analysis of the IR spectra of the mixed-peptide-lipid monolayer from different subphases points to the fact that the peptide monolayer exhibits different binding properties and activities towards  $\text{Cu}^{2+}$  and  $\text{Zn}^{2+}$  cations. The fluorescence spectroscopic studies discussed below also support this conclusion.

**Fluorescence spectroscopic studies:** Originally, we measured the UV/visible absorption spectra of the mixed-peptide monolayer directly at the air–water interface with metal cations present in subphases. However, no significant difference was observed for monolayers in subphases with metal cations compared with those in the pure water subphase, although it is known that many metal–protein or metal–peptide complexes exhibit charge-transfer absorption bands in the visible region. Possibly the extinction coefficient arising from the metal–peptide binding is too small to be detected, especially for the Langmuir monolayers.

We then employed fluorescence spectroscopy to study the complexation. A fluorescent lipid molecule 5-(octadecanoylamino) fluorescein (ODFL) was added to the peptide-lipid solutions at 1% molar ratio as a probe.<sup>[33, 34]</sup> Again, since it was found that the single peptide-lipid monolayers and the mixed monolayer exhibit very similar fluorescence properties upon binding with metal cations, only the results of the mixed-peptide-lipid monolayer are shown here. In Langmuir monolayers with pure water as the subphase, the fluorescence

intensity is highest before the compression or at the very early stage of compression (Figure 5, solid lines). With continuous compression of the monolayer, the fluorescence starts to decrease due to the aggregation of lipid molecules in the monolayer. In the  $K^+$  or  $Mg^{2+}$  subphase, the monolayer exhibits a very similar fluorescence change upon compression to that observed for the pure water subphase (data not shown here).

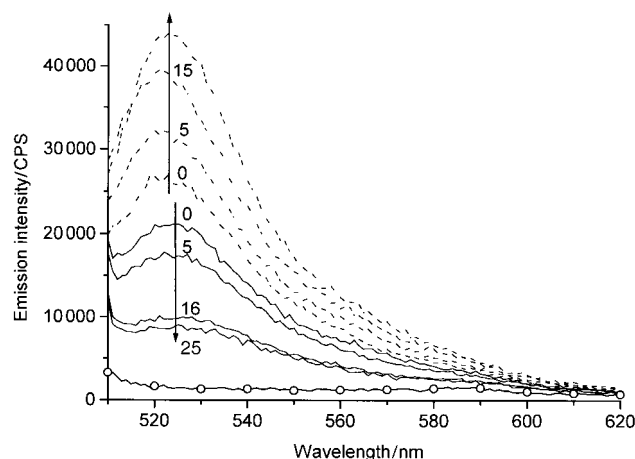


Figure 5. The fluorescence spectra (excitation 490 nm) of mixed-peptide-lipids monolayer at the air–water interface in pure water,  $ZnCl_2$  (1 mM), and  $CuCl_2$  ( $10^{-5}$  M) subphases. Fluorescent-probe ODFL was added to the peptide monolayer in 1% molar ratio: — water, ---  $ZnCl_2$ , -○-  $CuCl_2$ . The arrows indicate the direction in which the surface pressure (given in  $mN m^{-1}$ ) increases.

On the other hand, strikingly different fluorescence changes were obtained from  $Cu^{2+}$  and  $Zn^{2+}$  subphases. In the  $Cu^{2+}$  subphase with a concentration of  $10^{-5}$  M, the fluorescence is completely quenched (Figure 5, bottom) even before any compression. With continuous compression, no observable fluorescence was detected. However, in the  $Zn^{2+}$  subphase (1 mM), the monolayer exhibits the opposite fluorescence change to the pure water subphase. With continuous compression, the fluorescence intensity significantly increased with increased surface pressure (Figure 5, dashed lines). We noticed that if the concentration of  $Zn^{2+}$  is less than  $10^{-5}$  M, the fluorescence change of the monolayer is not so obvious; this suggests a much weaker binding between  $Zn^{2+}$  and peptides than between  $Cu^{2+}$  and peptides.

Further interesting fluorescence changes have been noticed with the binding and dissociation of  $Cu^{2+}$  from Langmuir–Schaefer films (touching deposition) of mixed-peptide-lipid monolayers. First, complete fluorescence quenching was observed from the one-layer Langmuir–Schaefer (LS) film deposited from a  $CuCl_2$  subphase ( $10^{-5}$  M, pH 5.9) at a surface pressure of  $15 mN m^{-1}$  onto a glass slide (Figure 6, solid line with open circle). The LS film was then dipped into a 0.01 N HCl solution for 5 min, rinsed with deionized water, and dipped in deionized water for another 5 min to obtain pH equilibrium. The fluorescence intensity from this film returned back to a value similar to the LS film obtained from the pure water subphase (Figure 6, dashed line with open circle). Then the film was dipped into a  $10^{-7}$  M  $Cu^{2+}$  solution for 5 min

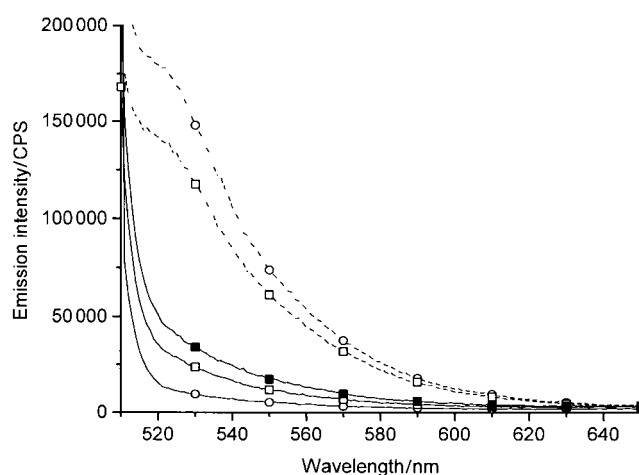


Figure 6. The reversible fluorescence spectral change (excitation 490 nm) of ODFL-labeled mixed-peptide-lipid Langmuir–Schaefer films upon binding with  $Cu^{2+}$  cations at different concentrations and dissociation with 0.01 N HCl. -○- deposited LS film from  $CuCl_2$  subphase ( $\times 10^{-5}$  M); --○-- washed with 0.01 N HCl, first time; -□- incubation in  $CuCl_2$  solution ( $\times 10^{-7}$  M) 5 min; --□-- washed with 0.01 N HCl, second time; -■- incubation in  $CuCl_2$  solution ( $\times 10^{-9}$  M) 10 min.

followed by rinsing with pure deionized water. Fluorescence quenching was again observed from the same film (Figure 6, solid line with open square). The same process was repeated for the same film and reversible fluorescence increase and quenching were observed repeatedly after washing the film with 0.01 N HCl (dashed line with open square) followed by incubation in  $CuCl_2$  solution at concentrations of  $10^{-9}$  (solid line with solid square) and  $10^{-11}$  M for 10–20 min. In  $Cu^{2+}$  solution at concentrations as low as  $10^{-13}$  M, after incubation for one hour about 50% fluorescence quenching was observed. Individually, all three peptide-lipid one-layer LS films were found to cause similar reversible fluorescence quenching/restoration as discussed here for mixed-peptide-lipid monolayers upon binding/dissociation with  $Cu^{2+}$ .

This result indicates that  $Cu^{2+}$  cations bound to the peptide monolayer when it was formed in the  $CuCl_2$  subphase and that the bound  $Cu^{2+}$  cations were dissociated from the binding sites when the binding sites were protonated under acidic conditions. It is impossible that the fluorescence increase or restoration of the peptide monolayer after incubation in acidic solution is due to the effect of protonation of the fluorescence probe ODFL itself, because the film was equilibrated in pure water for 5 minutes before spectra were taken and, furthermore, under acidic conditions the fluorescence from ODFL decreases rather than increases.<sup>[35]</sup> This result supports the previous suggestion that  $Cu^{2+}$  cations are complexed with the peptide monolayer through the imidazole nitrogen ligand from histidine. The  $pK_a$  of the histidine imidazole nitrogen is known to be around 6.0. In the pure water subphase with a pH around 6.0, about 50% of the imidazole groups are deprotonated; this makes these deprotonated nitrogens ready to complex with  $Cu^{2+}$ . Under acidic conditions, at pH 2.0, the protonated imidazole nitrogen is at an almost  $10^4$ -times greater concentration than the deprotonated; this leads to the observed dissociation of  $Cu^{2+}$  cations from peptide monolayer.

A general approach for developing fluorescent metal-cation sensors based on the complexation between peptides and metal cations is to attach a fluorescent probe covalently to a peptide known to complex with a specific metal cation.<sup>[17–21]</sup> The conformational change in the peptide introduces a conformational change in the fluorescence probe; this leads to a fluorescence change in the whole molecule. The interesting point about this new peptide monolayer/ $\text{Cu}^{2+}$  system is that the fluorescent lipid ODFL is only physically mixed with the peptide monolayer at 1%, but the binding activity of  $\text{Cu}^{2+}$  cations to the peptide monolayer is exceptionally high compared with some existing fluorescent probes for  $\text{Cu}^{2+}$ , such as GlyGlyHis derived with fluorescein isothiocyanate (FITC), which can only be used to detect  $\text{Cu}^{2+}$  cations at the submicron molar level.<sup>[36]</sup> GlyHisLys is another tripeptide that strongly binds with  $\text{Cu}^{2+}$  with a binding constant as high as  $10^{16} \text{ M}^{-1}$ , as mentioned in the introduction.<sup>[25–28]</sup> However, after attaching an anthracene group to the lysine-side-chain amino group, we could only observe obvious fluorescence quenching upon binding with  $\text{Cu}^{2+}$  at concentrations higher than  $10^{-7} \text{ M}$ .<sup>[37]</sup> A recently reported nonpeptide fluorescent sensor for aqueous  $\text{Cu}^{2+}$  from the combinatorial library approach requires 20 minutes of incubation to detect a  $\text{Cu}^{2+}$  concentration of  $5 \times 10^{-8} \text{ M}$ .<sup>[19]</sup> However, this work involves a much more complicated synthesis of ligand molecules for metal complexation.

We attempted to test the fluorescence reversibility of the mixed-peptide monolayer upon binding/dissociation with  $\text{Zn}^{2+}$ . At the same deposition surface pressure ( $15 \text{ mN m}^{-1}$ ), the fluorescence intensity of the monolayer film deposited from the  $\text{Zn}^{2+}$  (10 mM) subphase is much stronger than that of the pure water/monolayer film (Figure 7, solid lines with open and solid circle, respectively), corresponding to what was observed at the air–water interface. The film was then dipped into a 0.01 N HCl solution for five minutes followed by washing and incubation in pure water for five minutes. The fluorescence intensity of this film (Figure 7, thin dashed line) was found to decrease to a value approximately equivalent to that observed for the pure water/monolayer film; this indicated dissociation of  $\text{Zn}^{2+}$  from the monolayer. However, re-incubation of this film in  $\text{Zn}^{2+}$  solution, even at a concentration of 1 mM for 20 minutes, did not increase or restore the fluorescence intensity up to the value seen for the original  $\text{Zn}^{2+}$ -bound LS film (Figure 7, thick dotted line); this suggests an irreversible dissociation of  $\text{Zn}^{2+}$  from the peptide monolayer.

This different effect of  $\text{Cu}^{2+}$  and  $\text{Zn}^{2+}$  on the fluorescence change of the monolayer may reveal something about the different binding motifs of  $\text{Zn}^{2+}$  and  $\text{Cu}^{2+}$  to peptides. As dis-

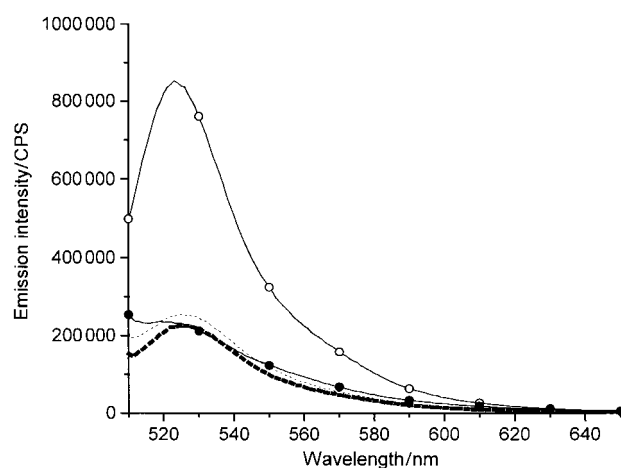


Figure 7. Fluorescence spectral change (excitation 490 nm) of ODFL-labeled mixed-peptide-lipid Langmuir–Schaefer films upon binding with  $\text{Zn}^{2+}$  cations and dissociation with 0.01 N HCl; compared with LS film deposited from pure water subphase. ○ film from  $\text{ZnCl}_2$  subphase, ---- washed with 0.01 N HCl, --- dipped in  $\text{ZnCl}_2$  solution (1 mM) 20 min, ● film from pure water subphase.

cussed for the IR spectra,  $\text{Zn}^{2+}$  complexation to the peptides is a weak binding and does not change the conformation of peptides significantly. Therefore, it is more likely that  $\text{Zn}^{2+}$  binds to the peptide monolayer by coordinating with imidazole groups from different peptides as shown in Figure 8a. In this configuration, the distance between fluorescence probe molecules is large enough, and fluorescence quenching due to close packing is inhibited. With continuous compression, we even observed the fluorescence increase of the monolayer (Figure 5) due to the lateral density increase. Upon protonation and dissociation of  $\text{Zn}^{2+}$  cations from the monolayer, the peptides interact together again possibly through hydrogen bonding to form a compact  $\beta$ -sheet structure, thus preventing reversible binding of  $\text{Zn}^{2+}$  to the monolayer.

On the other hand, binding of  $\text{Cu}^{2+}$  causes a reversible change of the peptide structure from  $\beta$ -sheet to turn. This

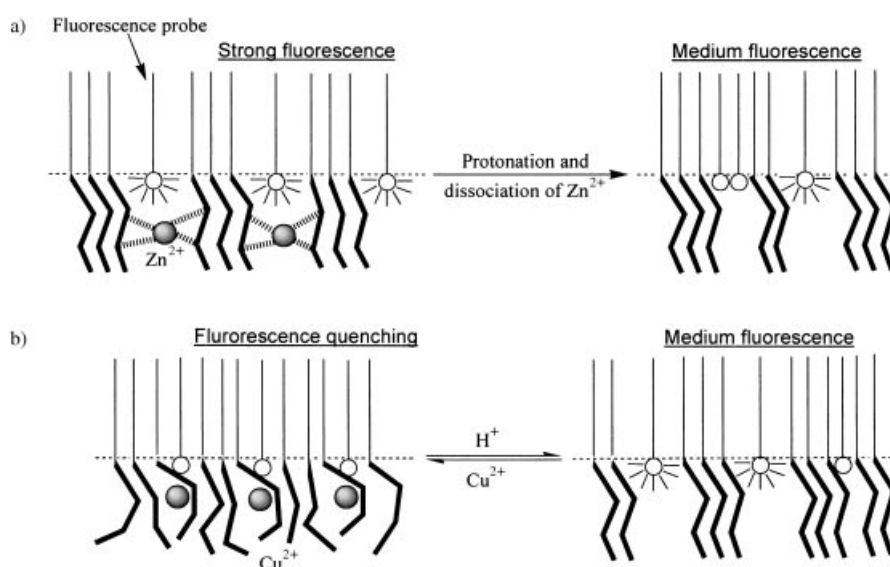


Figure 8. Models to explain the irreversible fluorescence increase (a) and reversible fluorescence quenching (b) of the mixed-peptide monolayers upon binding with  $\text{Zn}^{2+}$  and  $\text{Cu}^{2+}$ , respectively.

structural change probably results in some direct interactions between the fluorescein moiety and the  $\text{Cu}^{2+}$  cations or peptides, and leads to the fluorescence quenching (Figure 8b). Since the structural change is reversible, the fluorescence change is also reversible. At this stage of study, it is impossible to obtain a very clear model for describing the different binding mechanisms of  $\text{Cu}^{2+}$  and  $\text{Zn}^{2+}$  to the peptide monolayer. It would be ideal to examine the far-IR spectral region (lower than  $900\text{ cm}^{-1}$ ) to obtain metal–ligand coordination information; however, the band intensity of a one-layer LS film in this region is so weak that no conclusion can be drawn from the spectra. A more detailed analysis of the monolayer structures directly at the air–water interface by FT-IR spectroscopy is required for further investigations.

## Conclusion

In summary, we report here a new Langmuir monolayer system made from peptide or mixed-peptide lipids with metal complexation activity toward  $\text{Cu}^{2+}$  and  $\text{Zn}^{2+}$  cations. We reached an important conclusion that in Langmuir or Langmuir–Blodgett films peptides may adopt completely different secondary structures and exhibit different functions than in free solution; a behavior similar to proteins at the interfaces, but much less studied and understood. As a dynamic process, Langmuir monolayers provide a unique tool for controlling the assembling structure of lipid molecules at an interface and an alternate approach in the design and creation of novel two-dimensional molecular recognition systems. Metal complexation with peptides in free solution is a well-studied topic for bioinorganic chemists, and the investigation of this particular molecular recognition system at the interfaces may find some new potential applications in the development of nano-scale functional thin films or as biomimetic interfaces.

## Experimental Section

**The synthesis of peptide lipids PEP1 to PEP3:** Fmoc-protected amino acids and Rink resins were obtained from Advanced ChemTech. Other reagents, solvents, and stearic acid for the synthesis of peptide lipids were purchased from Aldrich. The synthesis of the three peptide lipids was accomplished by using solid-phase 9-fluorenylmethoxycarbonyl (Fmoc) chemistry with diisopropylcarbodiimide/1-hydroxybenzotriazole in situ activation. The coupling and deprotection cycle followed the literature procedure.<sup>[38, 39]</sup> Fmoc-protected amino acids were added to the Rink resin in fivefold molar excess to amino groups from the resin at a concentration of 0.3 M. After the coupling of the last amino acid residues, the resins were incubated overnight in a solution of the succinamidyl ester of stearic acid in dichloromethane at a concentration of 0.1 M. After being washed with dichloromethane and dried with methanol, the peptide lipids were cleaved from the resin by incubating the resin in  $\text{CF}_3\text{COOH}/\text{H}_2\text{O}$  (95:5, v/v) for two hours. The cleavage solution was concentrated in vacuo. The oil residue was precipitated from cold, deionized water, washed with cold, deionized water ( $5 \times$ ), benzene (once), and cold ether (once), and then centrifuged. After lyophilization, the product was used for the surface chemistry study without further purification. Analysis by HPLC indicated that the purity of each peptide lipid was more than 95%.

**Experimental conditions for surface chemistry studies:** HPLC-grade chloroform and methanol were obtained from Fisher Scientific. The peptide lipids were dissolved in chloroform/methanol (5:1, v/v) to a concentration of 1.0 mM and mixed together in 1:1:1 molar ratio as a mixture sample. The injected volumes were 25  $\mu\text{L}$  for mixed-peptide lipid samples and 60  $\mu\text{L}$  for pure lipid samples. After the sample had been spread, the solvent was allowed to evaporate for 15 min. The water used for the monolayer study was purified by a Modulab 2020 water purification system (Continental Water Systems Corp., San Antonio, TX). The water had a resistance of  $18\text{ M}\Omega\text{ cm}$  and a surface tension of  $72.6\text{ mN m}^{-1}$  at  $20^\circ\text{C}$ . The chlorides  $\text{CuCl}_2$ ,  $\text{ZnCl}_2$ ,  $\text{CdCl}_2$ ,  $\text{KCl}$ , and  $\text{MgCl}_2$  used for subphase preparation were purchased from Aldrich and were dissolved in deionized water to different concentrations. All the subphases were adjusted with 1 N NaOH or HCl solution to pH 6.0, if the pH of the metal subphases was not around this value. The adjusted subphases were allowed to stabilize in air for one to two hours before use. Since no buffer was used for the study, each subphase was freshly prepared before the experiment. The after-experiment test of the subphase indicated that the pH variation was less than 0.2 before and after experiments. The compression rate was set at  $4\text{ \AA}^2$  per molecule per minute for the surface pressure–area isotherm measurements.

All the experiments were conducted in a clean room class 1000 where the temperature ( $20 \pm 1^\circ\text{C}$ ) and the humidity ( $50 \pm 1\%$ ) were controlled. The Langmuir trough used for the surface pressure measurements was a KSV2000 mini-trough with dimensions  $7.5\text{ cm} \times 30\text{ cm}$ . The surface pressure was measured by the Wilhelmy method, the sensitivity of the Wilhelmy plate being  $\pm 0.01\text{ mN m}^{-1}$ . All the isotherm measurements were repeated three times, and the isotherms presented are the averages of these three measurements. The difference between the average isotherm and any of the three individual isotherms is  $\pm 1\text{ \AA}^2$  per molecule.

**FT-IR spectroscopic study of Langmuir–Blodgett films:** Mixed-peptide monolayers in water,  $\text{Cu}^{2+}$  ( $10^{-5}\text{ M}$ ), and  $\text{Zn}^{2+}$  ( $10^{-5}\text{ M}$ ) subphases were prepared and compressed to the surface pressures ready for deposition. The monolayers were transferred onto a gold-evaporated glass slide by vertical dipping to form one-monolayer LB films. (A gold layer 300 nm thick was deposited on a chromium layer, which stabilizes the gold layer during the evaporation process.) The Langmuir–Blodgett depositions were performed on a Kyowa Interface Science (Saitama, Japan) HBM LB film apparatus at  $25^\circ\text{C}$ . The subphase water was pure, with a pH of about 6.0. Infrared reflection-absorption (IRRA) spectra were measured by a Nicolet (Madison, WI) Magna 850 FT-IR spectrometer with a deuterated triglycine sulfate (DTGS) detector at a modulation frequency of 5 kHz. For the reflection measurements, a Harrick Scientific (Ossining, NY) RMA-1DG/VRA variable-angle reflection attachment was used in the FT-IR sample room. The angle of incidence was fixed at  $80^\circ$  from the surface normal. The p-polarized infrared ray for the IRRA measurements was generated through a Hitachi (Tokyo, Japan) wire-grid infrared polarizer made of AgBr. The measurement temperature was maintained at  $25^\circ\text{C}$ .

**Fluorescence spectroscopic studies:** The fluorescence emission spectra were recorded with a Spex Fluorolog 1680 spectrophotometer. For the measurement of emission spectra of the labeled monolayer directly at the air–water interface, an optical fiber probe with a probing area of  $0.25\text{ cm}^2$  was placed 1 mm above the water surface. The excitation light was transmitted through the optical fiber from the light source to the monolayer, and the emission light from the monolayer was also sent back to the detector through the optical fiber. For the measurement of fluorescence from Langmuir–Schaefer films, the monolayers were transferred to the hydrophobic glass slide by horizontal lifting. The glass slide used for the deposition was pre-cut to exactly fit the 1 cm fluorescence cuvette with an angle of  $45^\circ$  facing both the incidence and emission light beams to ensure the accuracy and reproducibility of each measurement.

## Acknowledgement

The authors thank the following for financial support: National Science Foundation, grant number CHE0091390, Department of Defense–US Army, contract number DAAD19-00-1-0138, Charles Culpeper Foundation, joint grant from the National Science Foundation of the United States and the Japan Society for the Promotion of Science for the support of the US–Japan Cooperative Research Program.



- [1] D. Möbius, R. Miller, *Proteins at Liquid Interfaces* Elsevier, Amsterdam, **1998**.
- [2] T. A. Horbett, J. L. Brash, *Proteins at Interfaces II: Fundamentals and Applications* American Chemical Society, Washington, DC, **1995**.
- [3] S. F. Sui, H. Wu, Y. Guo, K. S. Chen, *J. Biochem.* **1994**, *116*, 482.
- [4] K. Fujita, S. Kimura, Y. Imanishi, E. Okamura, J. Umemura, *Langmuir* **1995**, *11*, 1675.
- [5] E. Terzi, G. Holzemann, J. Seelig, *Biochemistry* **1997**, *36*, 14845.
- [6] D. Dieudonne, A. Gericke, C. R. Flach, X. Jiang, R. S. Farid, R. Mendelsohn, *J. Am. Chem. Soc.* **1998**, *120*, 792.
- [7] W. F. DeGrado, J. D. Lear, *J. Am. Chem. Soc.* **1985**, *107*, 7684.
- [8] K. Ariga, T. Kunitake, *Acc. Chem. Res.* **1998**, *31*, 371.
- [9] T. Kunitake, *Pure Appl. Chem.* **1997**, *69*, 1999.
- [10] X. Cha, K. Ariga, M. Onda, T. Kunitake, *J. Am. Chem. Soc.* **1995**, *117*, 11833.
- [11] X. Cha, K. Ariga, T. Kunitake, *J. Am. Chem. Soc.* **1996**, *118*, 9545.
- [12] P. Berndt, G. B. Fields, M. Tirrell, *J. Am. Chem. Soc.* **1995**, *117*, 9515.
- [13] Y. C. Yu, P. Berndt, M. Tirrell, G. B. Fields, *J. Am. Chem. Soc.* **1996**, *118*, 12515.
- [14] Q. Huo, G. D. Sui, P. Kele, R. M. Leblanc, *Angew. Chem.* **2000**, *112*, 1934; *Angew. Chem. Int. Ed.* **2000**, *39*, 1854.
- [15] J. H. van Esch, R. J. M. Nolte, H. Ringsdorf, G. Wildburg, *Langmuir* **1994**, *10*, 1955.
- [16] L. Schmitt, T. M. Bohanon, S. Denzinger, H. Ringsdorf, R. Tampé, *Angew. Chem.* **1996**, *108*, 344; *Angew. Chem. Int. Ed. Eng.* **1996**, *35*, 317.
- [17] "Fluorescent and Photochemical Probes of Dynamic Biochemical Signals inside Living Cells" R. Y. Tsien in *Fluorescent Chemosensors for Ion and Molecule Recognition* (Ed.: A. W. Czarnik), ACS Symposium Series 538, American Chemical Society, Washington DC, **1992**, pp. 130–146.
- [18] H. A. Godwin, J. M. Berg, *J. Am. Chem. Soc.* **1996**, *118*, 6514.
- [19] A. Singh, Q. Yao, L. Tong, W. C. Still, D. Sames, *Tetrahedron Lett.* **2000**, *41*, 9601.
- [20] G. K. Walkup, B. Imperiali, *J. Am. Chem. Soc.* **1997**, *119*, 3443.
- [21] S. Bhattacharya, M. Thomas, *Tetrahedron Lett.* **2000**, *41*, 10313.
- [22] S. J. Lau, T. P. A. Kruck, B. Sarkar, *J. Biol. Chem.* **1974**, *249*, 5878.
- [23] P. F. Predki, C. Harford, P. Brar, B. Sarkar, *Biochem. J.* **1992**, *287*, 211.
- [24] R. W. Hay, M. M. Hassan, Y. Q. Chen, *Inorg. Chem.* **1993**, *32*, 17.
- [25] L. Pickart, M. M. Thaler, *Nature New Biol.* **1973**, *243*, 85.
- [26] L. Pickart, J. H. Freedman, W. J. Loker, K. Peisach, C. M. Perkins, R. E. Stenkamp, B. Weinstein, *Nature* **1980**, *288*, 715.
- [27] L. Pickart, S. Lovejoy, *Methods Enzymol.* **1987**, *147*, 314.
- [28] a) S. A. Daignault, A. P. Arnold, A. A. Isab, D. L. Rabenstein, *Inorg. Chem.* **1985**, *24*, 3984; b) M. J. Rainer, B. M. Rode, *Inorg. Chim. Acta* **1985**, *107*, 127; c) C. M. Perkins, N. J. Rose, B. Weinstein, *Inorg. Chim. Acta* **1984**, *82*, 93; d) M. J. Rainer, B. M. Rode, *Inorg. Chim. Acta* **1984**, *92*, 1; e) J.-P. Laussac, R. Haran, B. Sarkar, *Biochem. J.* **1983**, *209*, 533; f) J. H. Freedman, L. Pickart, B. Weinstein, W. B. Mims, J. Peisach, *Biochemistry* **1982**, *21*, 4540; g) S.-J. Lau, B. Sarkar, *Biochem. J.* **1981**, *199*, 649.
- [29] F. MacRitchie in *Physical Chemistry of Biological Interfaces* (Eds.: A. Baszkin, W. Norde), Marcel Dekker, New York, **2000**, Chapter 5.
- [30] A. W. Czarnik, S. H. DeWitt, *A Practical Guide to Combinatorial Chemistry*, American Chemical Society, Washington DC, **1997**.
- [31] S. J. Lippard, J. M. Berg, *Principles of Bioinorganic Chemistry*, University Science Books, Mill Valley, CA, **1994**, p. 22.
- [32] B. R. Singh in *Infrared Analysis of Peptides and Proteins* (Ed. B. R. Singh), Chapter I: a) pp. 16–21; b) pp. 22–23; c) p. 41.
- [33] A. K. Dutta, C. Salesse, *Langmuir* **1997**, *13*, 5401.
- [34] J. Orbulescu, S. V. Mello, Q. Huo, G. Sui, P. Kele, R. M. Leblanc, *Langmuir* **2001**, *17*, 1525.
- [35] R. P. Haugland in *Handbook of Fluorescent Probes and Research Chemicals*, 6th ed. (Ed.: M. T. Z. Spence), Molecular Probe, Eugene, OR, **1996**, pp. 19 and 23.
- [36] R. P. Haugland in *Handbook of Fluorescent Probes and Research Chemicals*, 6th ed. (Ed.: M. T. Z. Spence), Molecular Probe, Eugene, OR, **1996**, p. 534.
- [37] Y. Zheng, Q. Huo, P. Kele, F. M. Andreopoulos, S. M. Pham, R. M. Leblanc, *Org. Lett.* **2001**, in press.
- [38] G. B. Fields, R. L. Noble, *Int. J. Peptide Protein Res.* **1990**, *35*, 161.
- [39] D. A. Wellings, E. Atherton in *Methods in Enzymology Vol 289: Solid Phase Peptide Synthesis* (Ed. G. B. Fields), Academic Press, New York, **1997**, pp. 44–67.

Received: October 6, 2000

Revised: June 11, 2001 [F3171]